

Shubnikov-de Haas Measurements in Bismuth

Rodney D. Brown, III

IBM Watson Laboratory, Columbia University, New York, New York 10025

(Received 18 November 1969)

The oscillatory transverse magnetoresistance (Shubnikov-de Haas effect) has been measured for the magnetic field in the binary and trigonal planes of single-crystal bismuth at liquid-helium temperatures, using a technique which permits accurate identification and determination of the periods and measurement of the amplitudes. Periods observed in high-purity samples [resistivity ratios ($R_{300\text{ }^\circ\text{K}}/R_{4.2\text{ }^\circ\text{K}}\rangle > 400$) can be fit to the generally accepted Fermi-surface model of one hole ellipsoid and three tilted electron ellipsoids. For resistivity ratios $\lesssim 300$, additional periods are observed which recently have been shown to be caused by twinning. The effects of twinning, together with the difficulty in interpreting oscillatory resistivity data taken by traditional techniques, are suggested as explanations for the many spurious periods reported in the literature and used as arguments for additional pieces of the Fermi surface. By fitting the amplitudes of the oscillations to the theory for the magnetoresistance of an electron gas with level (Dingle) broadening, the Dingle temperatures of holes and electrons were found to be (0.7 ± 0.2) and $(0.4 \pm 0.1)^\circ\text{K}$, respectively. These values are comparable with earlier results of Bhargava from de Haas-van Alphen (thermodynamic as opposed to transport) measurements, but are 50 times larger than the values estimated from zero-field conductivity. Agreement within a factor of 2 is obtained when the increased scattering of carriers in the highest Landau level, due to their low velocities along the magnetic field, is considered.

INTRODUCTION

The thermodynamic and transport properties of many solids, when measured as functions of an applied magnetic field, have components periodic in reciprocal magnetic field. Such effects were first observed by Shubnikov and de Haas (SdH) in the magnetoresistance¹ and by de Haas and van Alphen (dHvA) in the susceptibility² of bismuth at very low temperatures. Shortly thereafter, Landau³ showed these effects to be related to the quantization of the electronic motion transverse to the field which causes singularities in the density of states of the electron gas. A stimulus for the many recent investigations of these effects⁴⁻⁷ was the work of Onsager,⁸ who showed that the period P of the oscillation is simply related to the extremal cross-sectional area S of the Fermi surface normal to the magnetic field by $P = 2\pi e/\hbar c S$.

The oscillations increase in amplitude as the temperature is decreased and are usually observable only near liquid-helium temperatures. However, at the lowest temperatures the amplitude is limited by the intrinsic width of the Landau levels, determined by collision broadening. The theory was first discussed by Dingle,⁹ who showed that the broadening is equivalent to an increase in temperature by an amount T_D , the "Dingle" temperature.

Though the Fermi surface for bismuth is now

well known,^{10,11} there have been many reports in the literature¹²⁻¹⁶ of periods observed by the SdH effect which are inconsistent with the known Fermi surface. In addition, there has been no systematic study of the dependence of the amplitudes of the oscillations on magnetic field and on temperature, though one report¹¹ indicates that the Dingle temperature is approximately 50 times the value expected from a naive estimate. We report here the results of a detailed study of the oscillatory magnetoresistance of bismuth as a function of temperature, magnetic field, and crystal perfection, in order to resolve the above two inconsistencies. These studies depend largely on novel measurement techniques,^{17,18} which permit unambiguous identification of interfering oscillations and accurate measurements of their periods and amplitudes.

THEORETICAL BACKGROUND

Single Band

The theory for the motion of electrons in a magnetic field has been reviewed by many authors.¹⁹⁻²³ The transverse magnetoconductivity of a single band, taking account of collision broadening, has been treated rigorously by Miyake²⁴ and by Kubo *et al.*^{21,25} For a constant Fermi energy E_F their results for the transverse conductivity σ_{\perp} , including spin,²⁶ are

$$\begin{aligned} \sigma_{\perp} = & \frac{n_0 e^2}{m^* \omega_c^2 \tau_0} \left\{ 1 + \frac{5}{2} \left(\frac{\hbar \omega_c}{2E_F} \right)^{1/2} \sum_{r=1}^{\infty} \frac{(-1)^r}{r^{1/2}} \theta_r \exp\left(-\frac{2\pi r \Gamma}{\hbar \omega_c}\right) s \left(\frac{2\pi r E_F}{\hbar \omega_c} - \frac{\pi}{4} \right) \cos \pi \nu r \right. \\ & - \frac{3}{4} \frac{\hbar \omega_c}{2E_F} \ln \left[1 - \exp\left(-\frac{4\pi \Gamma}{\hbar \omega_c}\right) \right] + \frac{3}{2} \frac{\hbar \omega_c}{2E_F} \sum_{r=1}^{\infty} (-1)^r A_r \theta_r \exp\left(-\frac{2\pi r \Gamma}{\hbar \omega_c}\right) \cos\left(\frac{2\pi r E_F}{\hbar \omega_c}\right) \cos \pi \nu r \\ & \left. + \frac{3}{4} \frac{\hbar \omega_c}{2E_F} \sum_{r=2}^{\infty} (-1)^r B_r \theta_r \exp\left(-\frac{2\pi r \Gamma}{\hbar \omega_c}\right) \sin\left(\frac{2\pi r E_F}{\hbar \omega_c}\right) \cos \pi \nu r \right\}, \end{aligned} \quad (1)$$

where

$$\theta_r = \left[\frac{2\pi^2 r k T / \hbar \omega_c}{\sinh(2\pi^2 r k T / \hbar \omega_c)} \right], \quad (2)$$

$$A_r = \sum_{s=1}^{\infty} \left[\frac{\exp(-4\pi \Gamma / \hbar \omega_c)}{s^{1/2} (r+s)^{1/2}} \right], \quad (3)$$

and

$$B_r = \sum_{s=1}^{r-1} s^{-1/2} (r-s)^{-1/2}. \quad (4)$$

In the above equations, θ_r is a thermal factor, τ_0 the mean free time between collisions in the absence of the magnetic field, T the temperature, and $\omega_c = eH/m_c c$ the cyclotron frequency. Γ , the width of the Landau levels due to collision broadening, is itself an oscillatory function of the magnetic field since the scattering depends on both the density of states at the Fermi energy and the electron velocity, of which the component along the field approaches zero when a Landau level is at the Fermi surface. For $\Gamma \ll E_F$ and E_F constant, Γ is given by²⁴

$$\begin{aligned} \Gamma = & \frac{\hbar}{2\tau_0} \left[1 + \left(\frac{\hbar \omega_c}{2E_F} \right)^{1/2} \sum_{r=1}^{\infty} \frac{(-1)^r}{r^{1/2}} \right. \\ & \left. \times \exp\left(-\frac{2\pi r \Gamma}{\hbar \omega_c}\right) \cos\left(\frac{2\pi r E_F}{\hbar \omega_c} - \frac{\pi}{4}\right) \right]. \end{aligned} \quad (5)$$

At low fields, $\sinh(2\pi^2 k T / \hbar \omega_c)$ in Eq. (2) can be replaced by $e^{-2\pi^2 k T / \hbar \omega_c}$, and a Dingle temperature $T_D = \Gamma / \pi k$ can be defined which will add to the real temperature in θ_r .⁹ For large H , though this approximation does not hold, one can still regard Γ as an effective temperature T_D .

The first two terms in Eq. (1) are results of scattering between Landau levels and the last three terms are results of scattering within a level. In the limit $\Gamma \rightarrow 0$, the third and fourth terms will diverge. This divergence was first discussed by Davydov and Pomeranchuk,²⁷ who pointed out that the expected value of $\Gamma_0 = \hbar / \tau_0$ must be modified when the quantization alters the time the electron

spends in the neighborhood of a scattering center.

Application to Bismuth

Bismuth is a group-V semimetal having a rhombohedral crystal structure, with two atoms per unit cell.²⁸ The structure is a slight distortion of a face-centered cubic lattice, obtained by elongation along a body diagonal, the trigonal (z) axis. One of the three remaining twofold rotational axes is defined as a binary (x) axis; the bisectrix (y) axis is a third orthogonal axis. The slight distortion causes an overlap of the fifth and sixth Brillouin zones so that some of the 10 electrons per unit cell in the otherwise filled fifth zone go over into the sixth zone, creating equal electron and hole densities of 3×10^{17} per cm^3 at low temperatures. The electron Fermi surface^{10,11} consists of six half-ellipsoids at the L points in the zone; a principal axis of each of these ellipsoids is along an axis of twofold symmetry (the binary), the other two axes are tilted from the trigonal by an angle of $+6^\circ$.²⁹ The hole surface^{10,11} consists of two half-ellipsoids of revolution about the trigonal axis centered at the T points.

For a single band, the resistivity ρ_{\perp} , the experimentally determined quantity, is proportional to σ_{\perp} at high fields.²² However, for the case of bismuth in which the densities of holes and electrons have been shown to be equal within 5%,^{11,17,30} $\rho_{\perp} \equiv \sigma_{\perp}^{-1}$, where σ_{\perp} is given by a sum of expressions like those in Eq. (1) for each piece of the Fermi surface. From Eq. (1), writing OT for the oscillatory terms, substituting $\rho_{\perp}^{(0)}$ for $m^*/n_0 e^2 \tau_0$, the zero-field component of the resistivity, and μ_{\perp} for $e\tau_0/m_c$, the average mobility transverse to the field (where m_c is the appropriate cyclotron mass), one can write

$$\rho_{\perp} = \rho_{\perp}^{(0)} (\mu_{\perp}^2 H^2 / c^2) (1 + \text{OT})^{-1}. \quad (6)$$

For amplitudes of the oscillatory terms $\ll 1$, the case for moderately high fields, i. e., $\omega\tau_0 > 1$ but $n = E_F / \hbar \omega_c$ not small,

$$\rho_{\perp} \approx \rho_{\perp}^{(0)} (\mu_{\perp}^2 H^2 / c^2) (1 - \text{OT}). \quad (7)$$

Thus, for bismuth, there will be a monotonic term

proportional to H^2 and the amplitudes of the oscillations will also be multiplied by a factor of H^2 . One should note that, in contrast to the case for a single band, the resistivity will be a minimum at the singularities in OT.

The above assumes both E_F and Dingle factor constant and should be applicable to bismuth for n large near E_F . However, when the separation of the levels becomes a significant fraction of E_F , the change in E_F must be taken into account and constant broadening cannot be assumed.

Despite these limitations there appear to be certain directions of the magnetic field in bismuth for which the above low-field theory may be used at higher fields. For example, for H along the binary, the cyclotron masses of the holes and of the electrons in one ellipsoid are relatively large ($0.14 m_0$ and $0.22 m_0$, respectively), while electrons in the other two ellipsoids have small cyclotron masses ($0.011 m_0$). For the two identical ellipsoids, the effect of H on E_F will be minimized. Smith *et al.*³¹ have calculated a maximum variation of approximately 2% in E_F for H along the three principal axes, for H up to 15 kG. The variation of Γ with H is taken into account through Eq. (5).

EXPERIMENTAL DETAILS

The apparatus and the method, described in detail previously,¹⁸ have two important features: First, the monotonic H^2 term in the magnetoresistance (Eq. 7) is subtracted by a bridge arrangement, allowing increased amplification of the oscillatory part, and second, the magnetic field is swept such that $1/H$ varies linearly with time, so that the oscillations are sinusoidal in time, making it possible to use real-time differentiators and filters to separate the periods. The periods (in $1/H$) are obtained directly from the recorder trace; averaging is accomplished by measuring over a number of periods. The accuracy of period measurements, from 1 to 10%, is determined by the magnetic field and sweep calibrations, sample orientation, the number of cycles observable, and distortion by other periods. For some directions of field (e.g., along the principal axes), the oscillations are unambiguous and exactly periodic; for others, the interpretation depends on having data at nearby directions. If the number (depending on the period) of well-resolved periods is sufficient, the field and sweep calibrations limit the accuracy to 1% between 2 and 13.5 kG. Orientation errors are at most 1% and, in general, are much less. The larger errors are due to a limited number of observable periods or to distortion by other periods.

For directions of the field in which the principal

harmonic of one period dominates and where the monotonic term is exactly cancelled, the amplitudes can be measured directly from the recorder traces. When higher harmonics become important, the amplitudes can be determined and the effect of imperfect cancellation of the monotonic term eliminated by fitting to an analytic expression for the oscillations derived from Eq. (6) [see Eq. (8)].

Sample Preparation

Samples were cut from large single crystals grown from 99.9999% pure zone-refined bismuth by a modified Bridgeman technique as described in Ref. 18. The resistivity ratio $R_{300^\circ\text{K}}/R_{4.2^\circ\text{K}}$, which was of the order of 200 after cutting and planning, could be increased to ~ 500 by annealing near the melting point for ~ 200 h. Current and potential leads were attached with Ceroseal 150 solder or a bismuth-cadmium eutectic. Sample data are found in Table I.

EXPERIMENTAL RESULTS

Periods

The angular variations of the periods of electrons and holes in the binary and trigonal planes were determined using samples 28-3-b and 10-b-1 in Table I. In the figures, A , D , and F_R indicate data taken using an amplifier, differentiator, and rejection filter, respectively. The period to which the filter is tuned is indicated in parentheses in units of 10^{-5} G^{-1} .

Examples of period data are shown in Figs. 1-3. Figure 1 shows the oscillatory part of the magnetoresistance (R_H^{osc}) of a trigonal sample plotted versus reciprocal field for the field along the bisectrix for three amplifier gains. The electron periods (8.05 and $4.02 \times 10^{-5} \text{ G}^{-1}$) are readily determined by direct measurements on the graph. Figure 2 shows similar data for the same sample, only now with the magnetic field direction -10° from the bisectrix. This is typical of data for which multiple periods due to different part of the Fermi surface are superimposed. The present technique is particularly useful for handling such data, and careful analysis¹⁸ allows us to associate each of the minima with the correct period or periods. For this case, the three electron periods are 2.81, 5.1, and $7.92 \times 10^{-5} \text{ G}^{-1}$.

Figure 3 shows the results of an attempt to observe the electron periods for H near the trigonal. (The period along the trigonal has been observed only recently in dHvA measurements.¹¹) The filter was tuned to reject the hole period (top curve); however, the remaining dominant oscillation was the hole second harmonic, as confirmed by observing the phase between the two traces for H in the bi-

TABLE I. Sample data and experimental results.

Sample	Dimensions (cm)			$R_{300^\circ\text{K}}/R_{4.2^\circ\text{K}}$	Periods (10^{-5} G^{-1})				Remarks
	x	y	z		Electrons		Holes		
10-b-1	0.38	0.35	4.00	190	x 7.05, 0.51	y 8.05, 4.02	x, y 0.48	z	Unannealed
28-3-b	4.66	0.46	0.51	200		8.23, 4.17	0.50	1.58, 8.0 ^a	Unannealed
II-1 ^b	5.00	0.28	0.25	160		8.30, 4.0		1.57, 7.9 ^a	Unannealed
II-Cy-2 ^b	dia.	0.71	3.54	460	7.0	8.06, 4.13			Annealed after cutting
II-G ^b	4.25	0.60	0.30	500		8.10, 4.02		1.57 ^c	Annealed after cutting
				Average	7.03, 0.51	8.15, 4.07	0.49	1.57	
				Errors	$\pm 0.07, 0.02$	0.10, 0.07	0.02	0.02	
Electron tilt angle								$+6^\circ$	
Carrier densities per ellipsoid									
Electron								$0.96 \pm 0.03 \times 10^{17}/\text{cm}^3$	
Holes								$2.91 \pm 0.12 \times 10^{17}/\text{cm}^3$	
Dingle temperature									
Electrons, binary direction, $P=7.0 \times 10^{-5} \text{ G}^{-1}$								$(0.7 \pm 0.2)^\circ\text{K}$	
Holes, trigonal direction, $P=1.57 \times 10^{-5} \text{ G}^{-1}$								$(0.4 \pm 0.1)^\circ\text{K}$	

^aTwin electron period.

^bCrystal II was grown by R. L. Hartman and sample II-Cy-2 prepared by him (cf. Ref. 34).

^cNo twin period observable.

nary plane within -20° – $+24^\circ$ of the trigonal direction. This illustrates a case where data over a range of angles were necessary for correct interpretation, since the minimum electron period near the trigonal in this plane is known to be about $0.7 \times 10^{-5} \text{ G}^{-1}$. The electron period could not be seen. However, a low-amplitude long-period ($\sim 8 \times 10^{-5} \text{ G}^{-1}$) oscillation was observed for H within 10° – 15° of the trigonal direction. The same oscillation with much greater amplitude was also observed in sample II-1.¹⁶ Other examples of data obtained with this method are found in Ref. 18.

Angular dependences of the electron and hole per-

iods in the binary plane are shown in Fig. 4. The large dots along curves 1 and 2 indicate the measured periods for the electron Fermi surface. The experimental errors along these curves range from $0.1 \times 10^{-5} \text{ G}^{-1}$ for the large periods to $0.05 \times 10^{-5} \text{ G}^{-1}$ for the shorter well-resolved periods. The accuracy is indicated either by dot sizes or error bars. The solid lines (1 and 2) were calculated from Ketterson and Eckstein's³² equations for an ellipsoidal surface using the measured values of the tilt angle,²⁹ the periods in the bisectrix direction (Table I), and Bhargava's¹¹ value for the electron

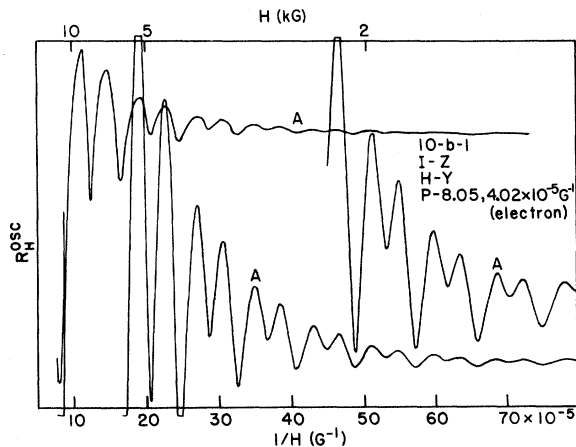


FIG. 1. SdH oscillations in a trigonal sample for H along the bisectrix at three amplifier gains.

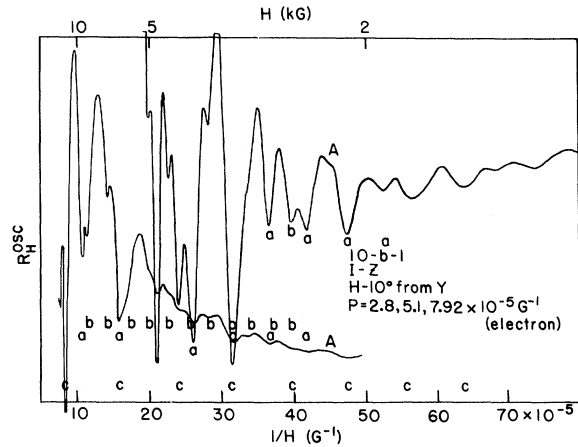


FIG. 2. SdH oscillations in a trigonal sample for H 10° from the bisectrix at two amplifier gains. a, b, and c indicate the locations of minima associated with the three observed periods.

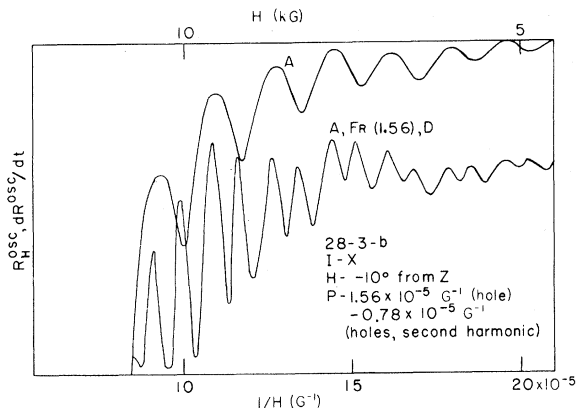


FIG. 3. SdH oscillations in a binary sample for $H - 10^\circ$ from the trigonal using the filter to reject hole period at $1.56 \times 10^{-5} \text{ G}^{-1}$, and the differentiator to bring out expected short electron period. The short period actually observed is the second harmonic of the hole period.

period in the trigonal direction $1.17 \times 10^{-5} \text{ G}^{-1}$. Two ellipsoids have the same variation of period with field (curve 2). The dots along curve 3 indicate the measured hole periods in this plane with an error of $\sim 0.02 \times 10^{-5} \text{ G}^{-1}$. The solid line is calculated from the ellipsoidal model using the mea-

sured values along the trigonal and bisectrix axes. The small dots indicate the second harmonic of the holes observed near the trigonal.

Crosses, triangles, and circles indicate periods that do not fit into the accepted Fermi surface of bismuth. The crosses might be explained by harmonics or by interference among the other oscillations; however, the circles and triangles along the trigonal would be hard to explain in this way, since the only periods of detectable amplitudes in this direction are due to the holes. These trigonal oscillations were observed in sample II-1 as a function of temperature.¹⁶ The temperature dependence of the amplitude gave an effective mass of approximately $0.010 m_0$. The same periods were also seen in dHvA measurements, using the technique described by Bhargava.¹¹ Data on these periods were not as good as those on the major periods, the error being of the order of $\pm 10\%$ due to the few low-amplitude cycles observable, and it was impossible to make a connection between these trigonal periods and the other unexplained periods in Fig. 4. In presenting a preliminary report¹⁶ on these data, it was learned that similar periods had been seen in other investigations.³³

We subsequently discovered that carefully annealed samples with resistivity ratios above ~ 400 did not show these periods. However, the periods

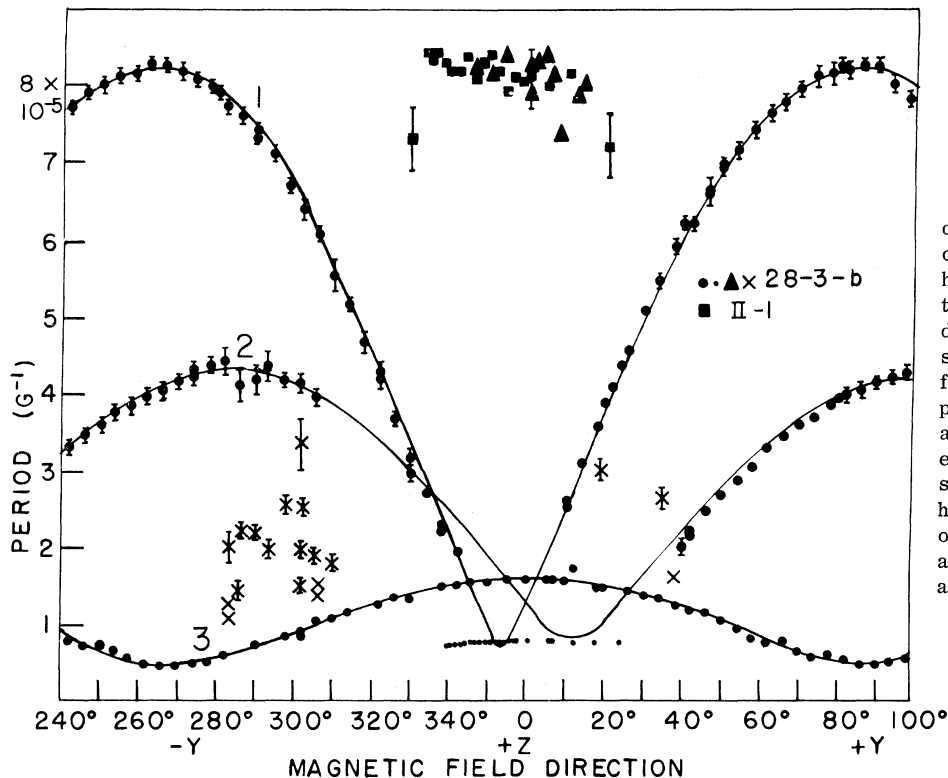


FIG. 4. Angular dependence of the electron periods (curves 1 and 2) and hole periods (curve 3) in the binary plane. Large dots are experimental points; solid lines are calculated from the periods along the principal axes and the tilt, assuming an ellipsoidal model; small dots indicate measurements of the second harmonics of the hole periods. Triangles, squares, and crosses are periods arising from twinning.

could be induced by straining (bending in a four-point jig at either room or helium temperatures) and eliminated by annealing near the bismuth melting point. For resistivity ratio increasing from ~ 250 to 400 , the amplitude of the period dropped by a factor of approximately 20. It was then learned³⁴ that these periods result from twinning.³⁵

Figure 5 shows the electron periods (curves 1–3) as functions of angle in the trigonal plane. Again the dots are the measured values and the solid lines are calculated from the periods along the principal axes. The errors range from about $0.1 \times 10^{-5} \text{ G}^{-1}$ for the large periods to about $0.03 \times 10^{-5} \text{ G}^{-1}$ for the smaller ones. A few periods are shifted off the curves because of the interference between oscillations. There is also a discrepancy near the binary axis for the small electron periods, which may be the effect of nonellipsoidicity or the flattening of the ends of the ellipsoid in the long direction. A similar effect was seen and discussed by Bhargava.¹¹ The isotropic hole period in this plane is shown along curve 4; the error is $\sim 0.02 \times 10^{-5} \text{ G}^{-1}$.

For samples with resistivity ratios between 160

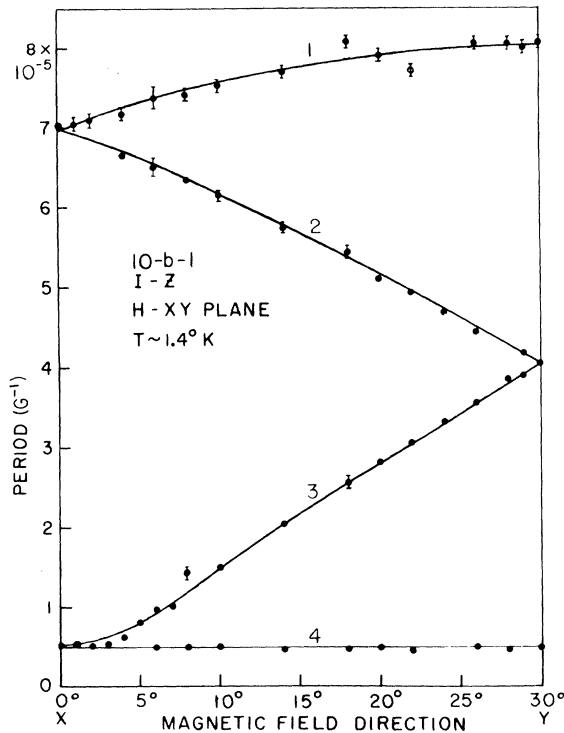


FIG. 5. Angular dependence of electron periods (curves 1–3) and hole periods (curve 4) in the trigonal plane. Dots indicate experimental data; solid lines are calculated from the periods along the principal axes, assuming an ellipsoidal model.

and 500 (Table I) the measured periods along the principal axes agree within experimental error.³⁶ The carrier densities per ellipsoid calculated from the averages of these periods are $n_e = (0.96 \pm 0.03) \times 10^{17} \text{ cm}^{-3}$, $n_p = (2.91 \pm 0.12) \times 10^{17} \text{ cm}^{-3}$. The ratio $n_p/n_e = 3.03$ is in better agreement with the model than one can expect from the uncertainties in the periods.

Dingle Temperature

Electrons

Careful measurement of the magnetic field dependence of the amplitudes of the oscillations was made on sample II-Cy-2 with H along the binary axis and the current along the trigonal axis, at temperatures between 1.4 and 4 °K. In this case the dominant oscillation, with period $7 \times 10^{-5} \text{ G}^{-1}$, is due to the electrons in two valleys which make identical contributions to the resistivity. Typical data are shown in Fig. 6. The Dingle temperature was determined by a self-consistent (computer) best fit of the envelope of the oscillations at the peaks and valleys of R_H^{osc} to the expression [cf. Eq. (6)]

$$R_H^{\text{osc}} = A \times H^p \times OT / (1 + OT), \quad (8)$$

where A depends on the sample parameters and gain of the measuring system and p is expected to be ~ 2 from Eq. (6). A and p are also determined from the fit; however, small variations in p have a substantial effect on the value T_D , with only a small change in the mean-square error in the fit. A first approximation to T_D could be obtained from the low-field region ($OT \ll 1$), where the sinh can be replaced by an exponential, assuming a value for p . A set of values for T_D spanning this value was then used to calculate $OT/(1+OT)$ with Γ given by an iterative solution to Eq. (5). In calculating OT for electrons, which have a nonparabolic energy dispersion,³⁷ the value of E_F in the argument of the cosine term in Eq. (1) was taken as that obtained by assuming equal spacing of the Landau levels with the cyclotron mass equal to the value at the Fermi energy. This “parabolic” E_F has a value of 15.8 meV.

The phase factor, $-\pi/4$ in Miyake’s expression, was experimentally close to zero as seen in Fig. 6 from the plot of the quantum number for each minima, which corresponds to an energy level at the Fermi surface, versus $1/H$. With the effective-spin factor ν assumed to be 2,³¹ a phase of $\sim -\pi/8$ gave the best calculated fit to the over-all shape of the oscillations, x points in Fig. 6. The quantity $OT/(1+OT)$ was then factored out of Eq. (8) and the values of A and p were determined from a least-squares fit to the remainder at various tem-

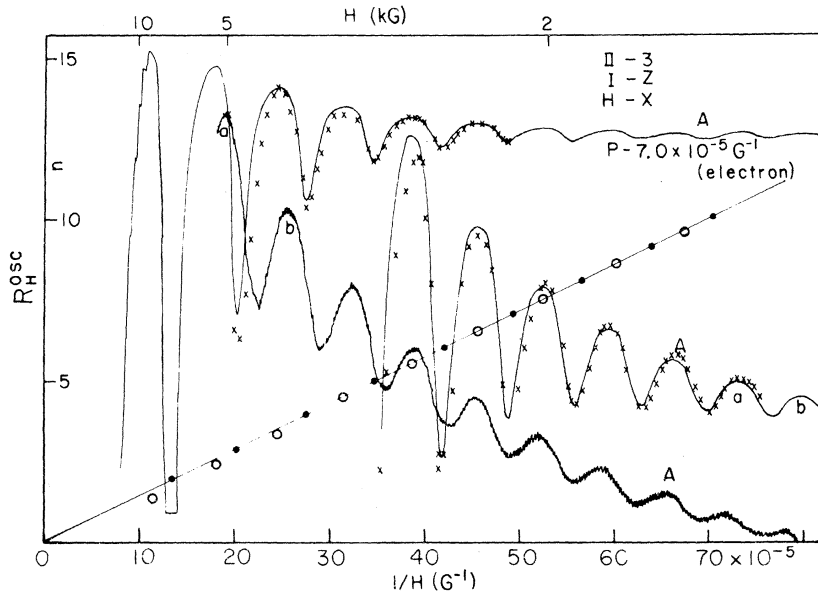


FIG. 6. Magnetic field dependence of the large-period electron oscillations for H along the binary. x 's indicate points calculated from Eq. (8) and Miyake's expression for OT; the straight line is a fit to the plot of the Landau-level numbers versus corresponding values of $1/H$ at the minima (dots), and indicates a phase close to zero; location of the maxima in $1/H$ are shown by circles.

peratures. The small monotonic term remaining in R_H^{osc} due to the imperfect cancellation of the H^2 term was eliminated by an iterative calculation which used the symmetry of the envelope function to determine the effective reference for the oscillatory terms. Since, as was mentioned above, near the minimum error small changes in T_D were compensated by changes in p (assuming p not to be a strong function of temperature), values of T_D for various ranges of p which gave errors near the minimum were obtained. For two ranges of p , 2.0 ± 0.1 and 2.25 ± 0.1 , these results are shown as a function of temperature in Fig. 7. For values of p very much outside these ranges, the error in the fit begins to increase significantly. From Fig. 7, assuming p independent of temperature, T_D ranges from $(0.7 \pm 0.2)^\circ\text{K}$ at $\sim 1.4^\circ\text{K}$ to $(0.4 \pm 0.2)^\circ\text{K}$ near 4°K . However, for a slight variation of p over this temperature range, a value of T_D $(0.6 \pm 0.2)^\circ\text{K}$ would be consistent with the data. Since the amplitudes are larger at lower temperatures, the best value for T_D is $(0.7 \pm 0.2)^\circ\text{K}$ at 1.4°K , for $p = 2.1 \pm 0.2$.

Holes

The amplitudes of the hole oscillations were measured as a function of magnetic field for field along the trigonal axis and current along the binary in sample II-G at temperatures between ~ 1.3 and 2.0°K . The same analysis described above was applied to these data, an example of which is shown in Fig. 8. In this case, since the spin factor ν of ~ 1 introduces a phase of $\sim \pi$ in the oscillations,

from the plot of level number versus $1/H$, Fig. 8, the phase factor in Miyake's expression Eq. (1) is ~ 0 . Since the minimum values of n observed for the holes were much larger than those for the electrons, the harmonics were of relatively lower amplitude and the exact phase was less critical and was assumed to be zero. For holes the best value of p was quite close to zero; the values of T_D versus temperature for three ranges of p are shown in Fig. 9. p and/or T_D are less dependent on temperature (assuming their dependencies do not cancel); the best value of T_D for holes is $(0.4 \pm 0.1)^\circ\text{K}$ for $p \sim 0$.

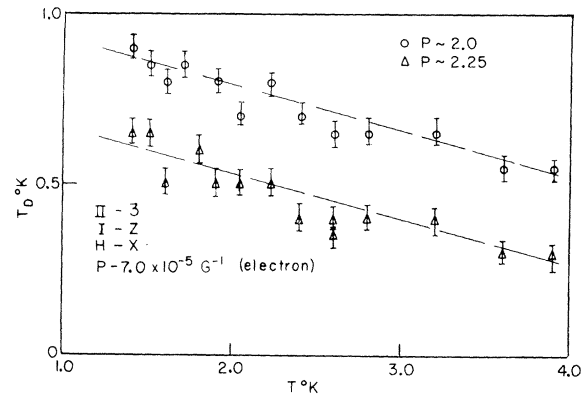


FIG. 7. Electron Dingle temperature for the large-period binary oscillations as a function of temperature for two ranges of p . Dashed lines are fit by eye to indicate the general trend.

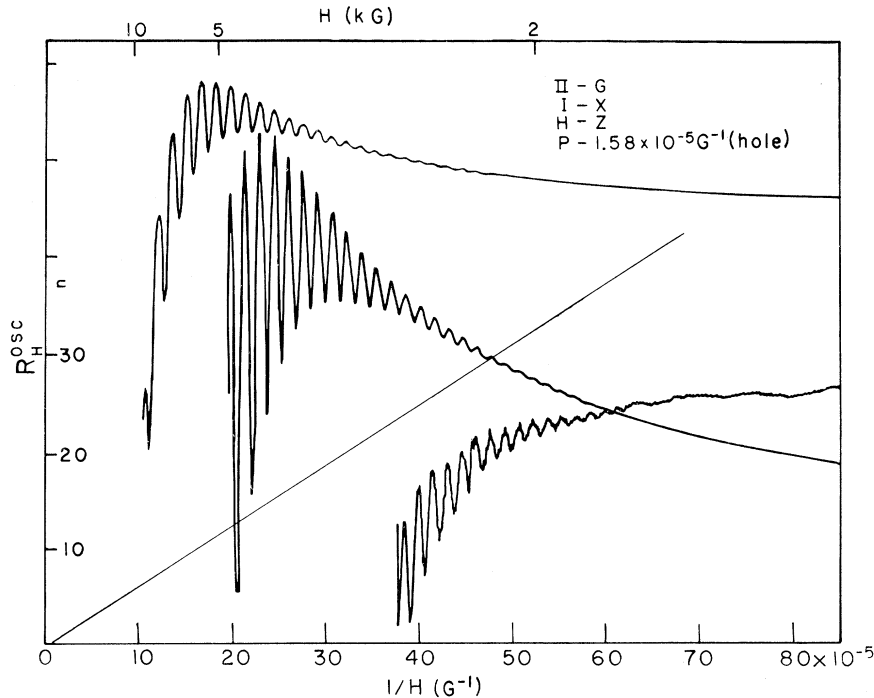


FIG. 8. Magnetic field dependence of hole oscillations for H along the trigonal. Straight line is a fit to the plot of Landau-level numbers versus values of $1/H$ at the minima, and indicates a phase (due in this case to spin) of $\pi/2$.

DISCUSSION

Periods

As seen from Figs. 4 and 5, the majority of the observed periods agree, within experimental error, with those expected from the known Fermi surfaces for the electrons and holes.³⁶ From the annealing data and Holland's x-ray and SdH results on strained crystals,³⁴ the periods near the trigonal axis (Fig. 4) are attributed to bisectrix periods

in a twin crystal. One of three possible orientations of the twin with respect to the parent³⁵ puts an angle of 116° between their positive trigonal axes,²⁹ with their binary axes along the same line but with opposite directions. This places the twin negative trigonal axis at approximately 284° in Fig. 4. The left-hand set of α points then corresponds to the expected electron periods obtained by shifting curve 1 by $\sim 74^\circ$ to the left. Some of the lower points near 280° are probably due to holes, as are the α points around 305° .

Since many of the data reported to date¹²⁻¹⁴ were taken on crystals for which the resistivity ratio ($R_{300^\circ\text{K}}/R_{4.2^\circ\text{K}}$) was 200 or less for crystals grown from fairly pure material, from the results indicated in Fig. 4 we would expect to see the effects of twinning in these data. The long anomalous period for magnetic field along the trigonal, now known to be due to twinning,³⁴ is, in fact, seen in the data of both Lerner¹² and Eckstein and Ketterson.¹⁴ It is clearly seen in Fig. 8 of Ref. 14 and can be estimated to be about $8 \times 10^{-5} \text{ G}^{-1}$; it is not quite so apparent in Lerner's data (Ref. 12, Fig. 4). In these cases we might expect to see spurious periods, especially short ones, either from the twin or from the additional interference between the twin and parent periods, particularly when recording the first or second derivatives of the magnetoresistance as a function of magnetic field. Lerner does report short periods, varying from 0.5 to $0.75 \times 10^{-5} \text{ G}^{-1}$ between the binary and bisec-

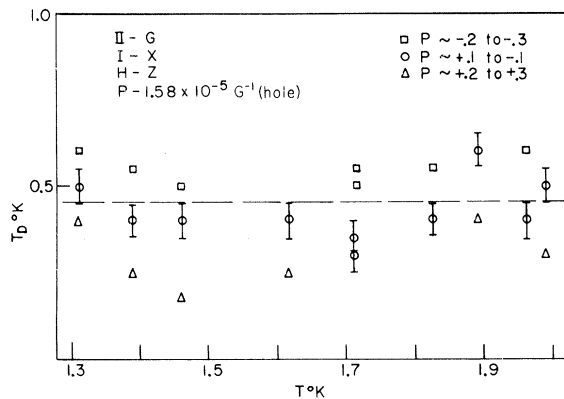


FIG. 9. Hole Dingle temperature for the trigonal oscillations as a function of temperature for three ranges of p . The dashed line is a fit by eye to show the general trend.

trix axes, which he attributes to a heavy hole band. Although Eckstein and Ketterson's samples had the lowest resistivity ratio, ~ 110 , they report very few periods, and no short ones, that do not agree fairly well with the accepted Fermi surface. Up to $\sim 10^\circ$ from the binary axis, Lerner's periods are quite close to our measured values of $0.5 \times 10^{-5} \text{ G}^{-1}$ for the isotropic hole period in the trigonal plane. In the region within $\sim 20^\circ$ of the bisectrix, the data are similar to those shown in Fig. 2 at 10° from the bisectrix, where it is quite difficult to separate the periods even for the undifferentiated data.

Balcombe and Forrest¹⁵ have reported direct measurements of the total magnetoresistance as a function of field on samples with reported resistivity ratios of 120, 300, and > 1000 . Their method of detection has inherently low sensitivity due to the large monotonic magnetoresistance of bismuth, and the data have a large amount of scatter. However, they do show that some of the periods observed by Lerner can be explained by the interference of the known periods in bismuth.

From our data, obtained by a method which reduces the possibility of interpreting interference peaks as spurious periods, from the analysis of Balcombe and Forrest,¹⁵ and from the effects that can be produced by twinning,³⁴ we conclude that there are no reported periods which cannot be interpreted in terms of the known band structure of bismuth.

Dingle Temperature

The measured values of the Dingle temperature for electrons along the binary, $\sim 0.7^\circ \text{K}$, and for holes along the trigonal $\sim 0.4^\circ \text{K}$ are in agreement with the previously reported values determined from dHvA measurements.¹¹ Using Hartman's³⁸ values of the average scattering times (τ_0) associated with the conductivity, and $\Gamma_0 = \hbar/\tau_0$, the expected values are ~ 0.01 and 0.007°K for electrons and holes, respectively. Thus, the measured values are approximately 65 times larger than this naive estimate. This discrepancy can be explained, however, and a close estimate of the Dingle factors can be obtained by an argument similar to that used by Davydov and Pomeranchuk²⁷ for estimating Γ . Their method is applicable to point scatterers of small cross section, for which each collision is considered an independent event, but in which case repetitive collisions occur because of the orbital motion and the low velocity in the z direction when a Landau level crosses the Fermi level. In the present case, because of its high dielectric constant ~ 100 ,³⁹ bismuth has a large Thomas-Fermi screening length, of the order of 500 \AA .⁴⁰ This is equal to the cyclotron radii of the electron and hole orbits for fields of 1000 and

2500 G, respectively, for H in the direction considered. Thus, for most of the above measurements, the orbit radius is of the order of or smaller than the screening length. When the orbiting electron encounters a scatterer as it drifts along H there will be a continuous interaction rather than the periodic one assumed by Davydov and Pomeranchuk. Since the scattering rate is proportional to the total time of the scattering interaction, which is inversely proportional to the velocity of the particle as it moves past the scatterer, an enhancement factor is obtained which will be given by the ratio of the velocity in the absence of the field (the Fermi velocity v_F) to that in the presence of the field v_z . The expression for τ becomes

$$1/\tau = (1/\tau_0) (v_F/v_z) = (1/\tau_0) (E_F/E_z)^{1/2}, \quad (9)$$

where E_z is the energy associated with the motion along H . Letting $\Gamma = \hbar/\tau$, and invoking the self-consistent relation^{24,27} $E_z = \Gamma$ (i. e., for the Landau level at E_F , E_z approaches zero within the width of the level), then

$$\Gamma = (\hbar/\tau_0) (E_F/\Gamma)^{1/2} \quad (10)$$

from which

$$\Gamma = \left(\frac{\hbar}{\tau_0} \right)^{2/3} (E_F)^{1/3} = \left(\frac{\hbar}{\tau_0} \right) \left(\frac{E_F}{\hbar/\tau_0} \right)^{1/3}. \quad (11)$$

From the values for E_F and τ_0 for the electrons and holes, the respective values of T_D from the last equation are 0.31 and 0.17°K . The agreement, within a factor of 2 of the measured values (Table I), is very good, considering the large initial discrepancy and the approximations of the model.

Comparison with Transport Theory

Electrons

The expression for the resistivity, Eq. (6) with OT given by Eq. (1), gives the correct general shape of the data for the large-period electron oscillations observed in the binary direction, for quite small values of n , when the experimentally observed nearly zero phase shift is inserted (cf. Fig. 6). The significant features are the sharp minima in the observed resistance, which according to Eqs. (1) and (6), correspond to density-of-states singularities at the Fermi level, and broadened maxima when the Fermi level lies between the singularities. By comparison with the results of Kunzler *et al.*⁵ on the oscillatory heat capacity, it is clear that the minima do in fact occur when the density-of-states singularities cross the Fermi energy. As discussed earlier, this is as expected for a semimetal with equal electron and hole densities when $\omega_c \tau > 1$ for both carriers, in contrast to the expectations for a carrier of one sign.

The above fit shows that the major contribution to the oscillatory magnetoresistance is due to the second term in Eq. (1), arising from collisions in which n changes. At high fields the effect of the oscillatory component in Γ is to increase the broadening at the minima and reduce it at the maxima. This results in a small oscillation in the logarithmic term and causes the amplitude at the minima to be smaller, and those at the maxima to be larger, than their values for constant Γ . The slight phase shift that is present, approximately $-\pi/8$, is responsible for the observed shifts of the peaks toward lower fields for $H > \text{kG}$ (Fig. 6).

The oscillatory terms [Eq. (1)] due to collisions in which n is constant begin to have significant amplitudes above $\sim 5 \text{ kG}$. However, the effect on the shape of the oscillations is slight for the phase, approximately zero. The fourth term has the same general effect as the second; the fifth term contributes to the second and higher harmonics, and its phase is such that were it present in greater amplitude, it would shift the peaks in the direction opposite to that observed. For the range of Dingle temperatures observed here, the logarithmic term in Eq. (1) has a maximum amplitude of about 25% of the first harmonic of the second term for $n=2$. Its principal effect is to add a small component to the monotonic background.

From Fig. 6 it can be seen that the minima of the oscillations have a constant period down to $n=2$. This is in contrast to Lerner's "class IV" oscillations (Ref. 12, Fig. 8) for magnetic field along the binary, which he finds aperiodic for $n < 7$. The "spiky" form of these oscillations seen by Lerner¹² and by Eckstein and Ketterson¹⁴ at high fields, using their derivative techniques, can be understood from the shape of the undifferentiated oscillations in Fig. 6. Since the maxima are broadened and are aperiodic at high fields, only the zero crossings in the derivative which are associated with the minima will be periodic.

Holes

In general, because of the higher cyclotron masses of the holes, the effect of the harmonics will be smaller than for the electrons. For electrons, at $n=6$ the ratio of the amplitudes of the second harmonic to the amplitude of the fundamen-

tal is 0.3; for holes, the ratio obtained from the best fit of the data to Eq. (6) is 0.08 and is in agreement with the data in Fig. 3, which yield 0.08 ± 0.02 for the ratio. At high fields, as seen in Fig. 3, the general shape is the same as for electrons. A phase of ~ 0 fits the data, assuming an effective-spin factor $\nu=1$.³¹ Since the harmonics have less effect and since the shape is difficult to determine for $n > 10$, no attempt was made to analyze the data with phase other than zero. In general, the peaks seem to be shifted toward lower fields, which would indicate a small negative phase factor.

We cannot explain the fact that the power of H in the factor multiplying the oscillatory terms is approximately 0, rather than 2, as found for electrons and expected for holes. A second unexplained feature of the data is the sharp decrease in the remaining monotonic term in the magnetoresistance which is observed above $\sim 5 \text{ kG}$, Fig. 8. The logarithmic term has the correct sign for the effect; however, its amplitude is too small ($\sim 10\%$ of that of the first harmonic at the highest fields in Fig. 8).

ACKNOWLEDGMENTS

My deepest thanks go to Dr. Seymour H. Koenig for suggesting this investigation, for illuminating many points of physics, and for his continued encouragement and patient guidance throughout the work; and to Professor Werner Brandt for his interest and helpful comments. I thank Dr. Rameshwar N. Bhargava for helpful discussions and aid in the early measurements; Dr. Alberto A. Lopez and Dr. Robert L. Hartman for helpful discussions, and the latter for the use of his bismuth crystal; Walter Schillinger for helpful discussions of the electronics; Dr. Alfred G. Redfield for the use of his magnet and laboratory facilities; Dr. Laura M. Roth for the loan of a copy of Miyake's thesis and a discussion of his results; and Professor R. N. Dexter and A. B. Holland for communicating their results on twinning prior to publication. I also thank the many members of the staff of Watson Laboratory who were of invaluable assistance; John Sierssen and the model shop staff, Joseph Cozzo and the electronic shop staff; and Mrs. Alice Kelbl for the drawings.

¹L. Shubnikov and W. J. de Haas, Leiden Commun. 207a (1930); 207c (1930); 207d (1930); 210a (1930).

²W. J. de Haas and P. M. van Alphen, Leiden Commun. 208d (1933); 212a (1933); 220d (1933).

³L. D. Landau, Z. Physik 64, 629 (1930).

⁴M. C. Steele and J. Babiskin, Phys. Rev. 98, 359 (1955).

⁵J. E. Kunzler, F. S. L. Hsu, and W. S. Boyle, Phys. Rev. 128, 1084 (1962).

⁶A. A. Lopez, Phys. Rev. 175, 823 (1968).

⁷B. A. Green and B. S. Chandrasekhar, Phys. Rev. Letters 11, 331 (1963).

⁸L. Onsager, Phil. Mag. 43, 1006 (1952).

⁹R. B. Dingle, Proc. Roy. Soc. (London) A211, 517

(1952).

¹⁰A. L. Jain and S. H. Koenig, *Phys. Rev.* **127**, 442 (1962).

¹¹R. N. Bhargava, *Phys. Rev.* **156**, 785 (1967).

¹²L. S. Lerner, *Phys. Rev.* **127**, 1480 (1962).

¹³L. S. Lerner, *Phys. Rev.* **130**, 605 (1963).

¹⁴Y. Eckstein and J. B. Ketterson, *Phys. Rev.* **137**, A1777 (1965).

¹⁵R. J. Balcombe and A. M. Forrest, *Phys. Rev.* **151**, 550 (1966).

¹⁶R. D. Brown, *Bull. Am. Phys. Soc.* **13**, 44 (1968).

¹⁷R. D. Brown, *Bull. Am. Phys. Soc.* **9**, 264 (1964).

¹⁸R. D. Brown, *IBM J. Res. Develop.* **10**, 462 (1966).

¹⁹A. H. Kahn and H. P. R. Frederikse, *Solid State Phys.* **9**, 257 (1959).

²⁰E. N. Adams and T. D. Holstein, *J. Phys. Chem. Solids* **10**, 254 (1959).

²¹R. Kubo, S. J. Miyake, and N. Hashitsume, *Solid State Phys.* **17**, 269 (1965).

²²L. M. Roth and P. N. Argyres, *Semicond. Semimet.* **1**, 159 (1966).

²³Comprehensive lists of references to previous work are contained in Refs. 19–22.

²⁴S. J. Miyake, thesis, Tokyo University, 1962 (unpublished).

²⁵An obvious error in Kubo's result has been corrected in Eq. (3). Equation (76) in Ref. 22 also contains errors.

²⁶R. B. Dingle, *Proc. Roy. Soc. (London)* **A211**, 500 (1952).

²⁷B. Davydov and I. Pomeranchuk, *J. Phys. (USSR)* **2**, 147 (1940).

²⁸W. S. Boyle and G. E. Smith, *Progr. Semicond.* **7**, 1 (1963).

²⁹R. D. Brown, R. L. Hartman, and S. H. Koenig, *Phys. Rev.* **172**, 598 (1968).

³⁰G. A. Williams, *Phys. Rev.* **139**, A771 (1965).

³¹G. E. Smith, G. A. Baraoff, and J. M. Rowell, *Phys. Rev.* **135**, A1118 (1964).

³²J. Ketterson and Y. Eckstein, *Phys. Rev.* **132**, 1885 (1963).

³³R. N. Dexter (private communication). Professor Dexter informed me that these periods had been seen in the course of investigations of the dHvA effect in uniaxially stressed bismuth [F. F. Huppe, thesis, University of Wisconsin, 1966 (unpublished)] and were being studied further by A. B. Holland. Huppe had measured approximately the same period, with the same effective mass, along the trigonal and was able to follow it further in angle in the binary plane where it fell off quite rapidly, and in fact, passed approximately through the x points in Fig. 4. These periods remained unexplained. However, Dexter speculated that they were due to imperfections in the sample.

³⁴A. B. Holland (private communication). Holland independently determined that these periods were associated with inelastic strain and showed from x-ray data that they were due to twinning, confirming Dexter's earlier speculation.

³⁵E. O. Hall, *Twinning* (Butterworths, London, 1961), p. 83.

³⁶See Ref. 11, Table I, for a list of periods reported by other investigators.

³⁷B. Lax, *Bull. Am. Phys. Soc.* **5**, 167 (1960); B. Lax, J. G. Mavroides, H. J. Zieger, and R. J. Noyes, *Phys. Rev. Letters* **5**, 241 (1960).

³⁸R. L. Hartman, *Phys. Rev.* **181**, 1070 (1969).

³⁹W. S. Boyle and A. D. Brailsford, *Phys. Rev.* **120**, 1943 (1960).

⁴⁰D. H. Brownell and E. H. Hygh, *Phys. Rev.* **164**, 909 (1967).

Optical Constants of Disordered Binary Alloys: Intraband Transitions in the Coherent-Potential Approximation*

B. Velicky[†] and K. Levin

Division of Engineering and Applied Physics, Harvard University, Cambridge, Massachusetts 02138

(Received 15 January 1970)

The optical constants of disordered binary alloys A_xB_{1-x} have been computed in the coherent-potential approximation for all frequencies, all x , and all reasonable scattering strengths, using a simple one-band model. Our results are compared with the classical Drude formula, and deviations are found stemming from critical points and the effects of alloying. In addition, the high-frequency behavior is shown to be dependent on the concentration x and scattering strength in the alloy.

I. INTRODUCTION

In the present paper the frequency-dependent conductivity $\sigma(\omega)$ of random binary alloys is calculated for all frequencies, all impurity concen-

trations, and a wide range of alloy scattering strengths. The coherent-potential approximation (CPA) is applied to the Kubo formula¹ for the complex frequency-dependent conductivity. This approximation has been shown^{2,3} to lead to easily